Springer

Journal of
Mechanical
Science and
Technology

Journal of Mechanical Science and Technology 22 (2008) 240~246

www.springerlink.com/content/1738-494x

Optimal contact design and allowable limit on spindle assembly of aluminum hot rolling process

Hyun-Seung Lee[1] and Young-Shin Lee[2,*]

[1]*BK21 Mechatronics Group, Dept. of Mechanical Design Eng., Chungnam National University 220 Gung-dong, Yu-seong, Dae-jeon, 305-764, Korea*

[2]*Director of BK21 Mechatronics Group, Department of Mechanical Design Engineering, Chungnam National University, 220 Gung-dong, Yu-seong, Dae-jeon, 305-764, Korea*

(Manuscript Received August 13, 2007; Revised November 15, 2007; Accepted November 22, 2007)

Abstract

Aluminum sheet ingots go through the hot rolling process to be converted into coils with a gauge suitable for the cold rolling process or plates. The top spindle, end coupling and slipper metal are main components of the hot roll process and used for transmission of rotational power with heavy-duty load. The top spindle connected to the motor and end coupling connected to the roller are combined with the slipper metal which acts as a bearing and joint. The contact surface between end coupling and slipper metal is subjected to stress concentration, and life cycles of slipper metal is reduced. This study aims to minimize the mechanical problems which might happen in the production process. The load condition for hot rolling processes is derived under load condition that is conducted for a hot rolling process under slipper metal combination types and operation situations. A structural analysis is performed by applying mechanical characteristics, combination type, and rotational boundary condition of top spindle, end coupling and slipper metal. Optimal design is performed for contact surface between end coupling and slipper metal. Interference analysis is studied to reduce the stress concentrations. Kinematics simulation is performed by applying the various combination type and dynamic boundary condition of the mill spindle assembly. The interference does not occur on the top spindle and slipper metal, so actual driving of the hot mill spindle assembly can operate in the normal operation condition.

Keywords: Rolling process; Optimal design; Spindle assembly; Allowable limit

---

1. Introduction

Hot rolling is the process of forming aluminum sheets from slab ingots that are up to 26 inches thick, 20 feet long, and weigh up to 20 tons. This ingot is then heated to around 500°C and passed several times through the hot rolling mill. The slab is heated in a furnace and rolled between powered rollers until the plate is approximately 1 inch thick. The plates are further reduced in finishing mills where they are hot rolled to a thickness of 0.25 - 0.4 inch. This thinner aluminum is then coiled and transported to the cold rolling mill for further processing. The top spindle connected to the motor and end coupling connected to the roller are combined with the slipper metal which act as bearing and joint[1-4]. The life cycles of slipper metal are reduced by the contact surface damage. Fig. 1 and Fig. 2 show an illustration of contact surface damage. Fig. 1 shows of damaged slipper metal under stress concentration. Fig. 2 shows the configuration of damaged slipper metal caused by wear. In this study, the structural analysis of a hot mill spindle assembly is carried out by using a commercial code ANSYS 8.0. Kinematics simulation is performed by applying the various driving angle and dynamic boundary conditions of the hot mill spindle assembly.

*Corresponding author. Tel.: +82 42 821 6644, Fax.: +82 42 821 8894
E-mail address: leeys@cnu.ac.kr
DOI 10.1007/s12206-007-1111-9

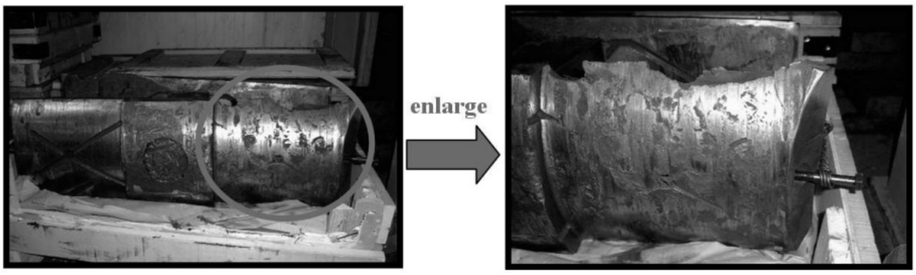

Fig. 1. Configuration of damaged slipper metal under stress concentration.

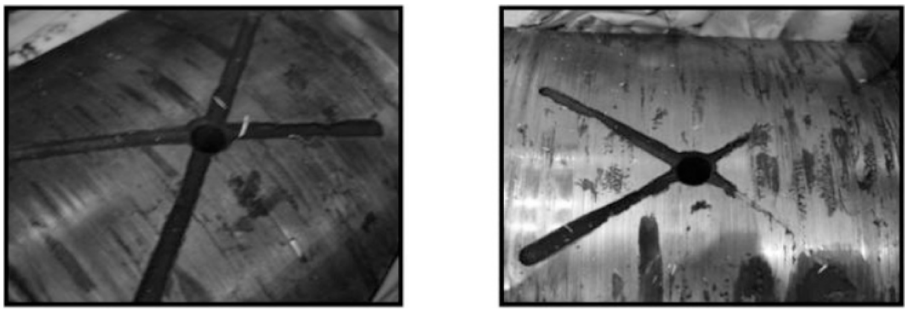

(a) Shape of slipper metal before wear (b) Shape of slipper metal after wear

Fig. 2. Configuration of damaged slipper metal caused by wear.

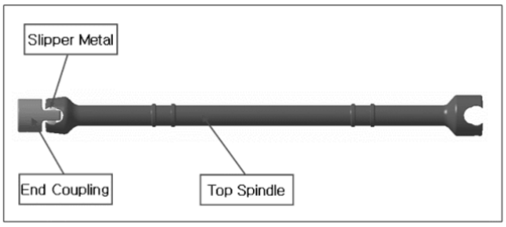

Fig. 3. Combination structure of the spindle assembly.

Fig. 4. Shape of top spindle.

This study focuses on optimal design and allowable limit on spindle assembly of AL hot rolling process under heavy duty load to minimize stress.

2. Optimal design of spindle assembly

2.1 Analysis model

Fig. 3 shows the combination structure of a hot mill spindle assembly. The spindle assembly consists of three components. Figs. 4-6 show components of the spindle assembly. Fig. 4 shows the shape of the top spindle. Fig. 5 shows the shape of the end coupling. The shape of the slipper metal is shown in Fig. 6. The

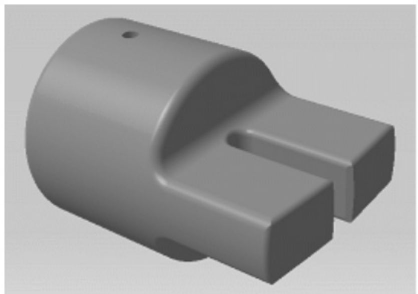

Fig. 5. Shape of end coupling.

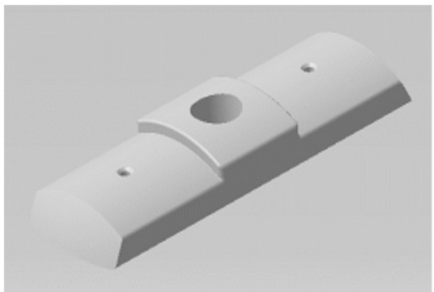

Fig. 6. Shape of slipper metal.

Table 1. Mechanical properties of SNCM-8.

Part	Top spindle, End coupling
Young's Modulus	205 GPa
Poisson' ratio	0.29
Density	7850 kg/m^3
Yield strength	1000 MPa
Tensile strength	1200 MPa

Table 2. Mechanical properties of ALBC-3.

Part	Slipper metal
Young's Modulus	100 GPa
Poisson ratio	0.23
Density	8930 kg/m^3
Yield strength	470 MPa
Tensile strength	588 MPa

mechanical properties of SNCM-8 steel for top spindle and end coupling are shown in Table 1. Table 2 shows the mechanical properties of ALBC-3 for slipper metal

2.2 Structural analysis of spindle assembly

The stress analysis of the spindle assembly is carried out by commercial FEM code ANSYS 8.0 with solid92. Solid92 has quadratic displacement behavior and is well suited to model irregular meshes such as produced from CAD data. The element is defined by ten nodes having three degrees of freedom at each node. The element also has plasticity, creep, swelling, stress stiffening, large deflection, and large strain capabilities. Fig.7 shows the configuration of the solid 92[5].

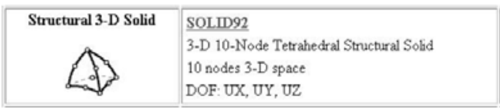

Fig. 7. Configuration of solid 92 element.

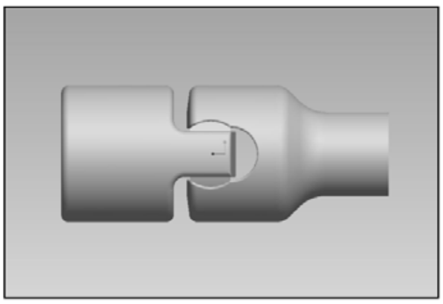

Fig. 8. Geometric model of spindle assembly.

The geometric model of the spindle assembly makes use of the commercial 3D CAD program. Fig. 8 shows a geometric model of spindle assembly. The FE model of the spindle assembly makes use of FEM code ANSYS 8.0. The configuration of the FE model is shown in Fig. 9. The finite element model of the hot mill spindle assembly is composed of 350000-elements and 400000-nodes. The maximum torques occurred by moment when the slab passed in the roller. The maximum torque is in 3000 kN · m under 150 percentage of motor generating power.

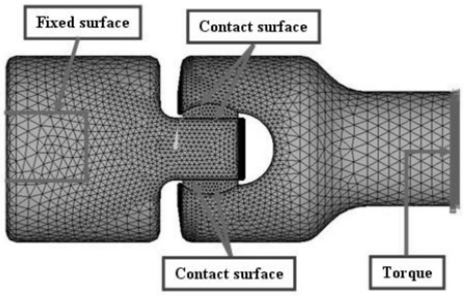

Fig. 9. FE model of spindle assembly.

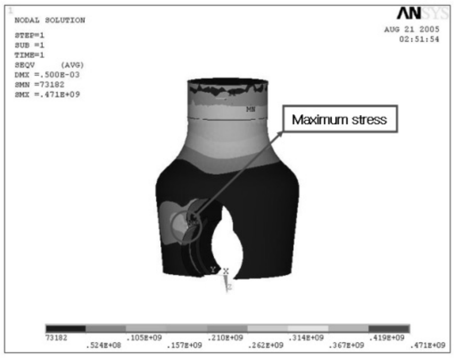

Fig. 10. Stress contour of the top spindle.

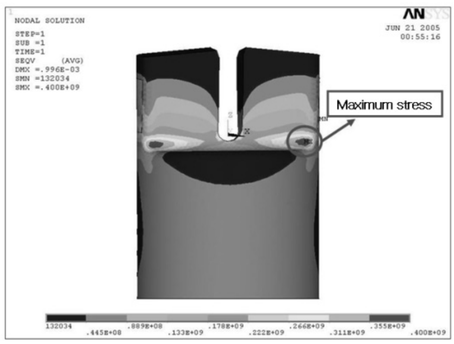

Fig. 11. Stress contour of the end coupling.

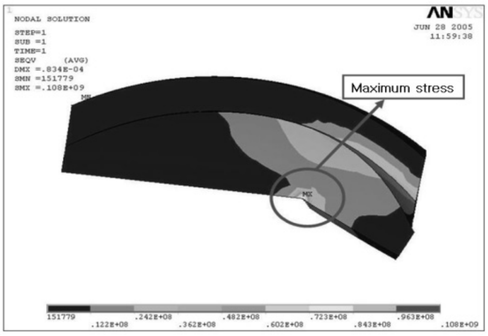

Fig. 12. Stress contour of the slipper metal.

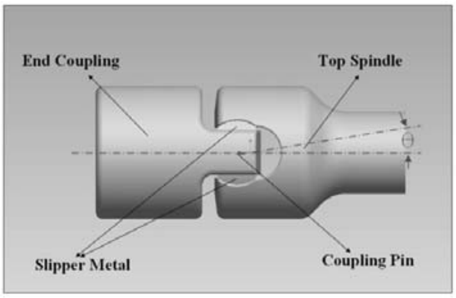

Fig. 13. Schematic diagram for combination structure of the top spindle, end coupling and slipper metal.

Fig. 14. Configuration of actual drive shape according to assembled angle with 2.97°.

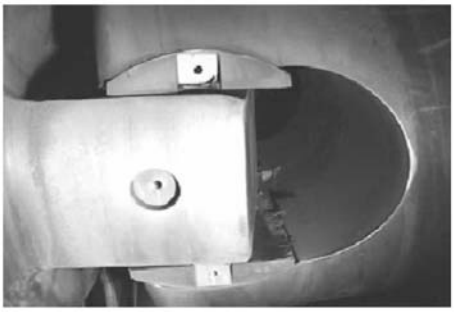

Fig. 15. Configuration of actual drive shape according to assembled angle with 6.70°.

Fig. 10 shows the stress contour plot of the top spindle. The stress contour plot of the end coupling is shown in Fig. 11 and that of the slipper metal is shown in Fig 12. From the results of structure analysis for spindle assembly, the stress concentration occurred in the slipper metal. This is because the hot rolling process changes the combination angle of the top spindle according to thickness of slab from 2.97° to 6.70°. Fig. 13 shows the combination structure of the hot mill spindle assembly. "θ" represents the combination angle of the top spindle. Stress concentration and contact damage occurring on the slipper metal due to the contact surface inconsistency between end coupling and slipper metal. The damage level will be increased with operation angle due to higher misalignment of the hot mill spindle assembly. Fig. 14 the shows actual drive shape according to assembled angle with 2.97°. Actual operation shape according to driving angle with 6.70° is shown in Fig. 15.

2.3 Shape optimization of spindle assembly

The size optimization analysis is carried out by the sub-problem method of ANSYS for design variables[6, 7]. Table 3 shows the optimization statement of the hot mill spindle assembly. The material of the top spindle and end coupling has a yield strength of 1000 MPa and a minimum ultimate tensile strength of 1200 MPa. Allowable strength of the top spindle and end coupling has 500 MPa with safe factor 2.0. The results of the optimization analysis for the hot mill spindle assembly, optimal designs of top spindle and end coupling are shown in table 4. Fig. 16 shows stress contour of optimized top spindle. Fig. 17 shows stress contour of optimized end coupling. Results of structural analysis for slipper metal are shown in Fig. 18. However, if the maximum stress of optimized end coupling is increased, the value is very small. From the optimization analysis, the maximum stress of the slipper metal according to a uniformly distributed load P decreased rapidly.

Table 3. Optimization statement of hot spindle assembly.

Method	Sub-problem approximation method	
Objective	Minimize stress of spindle metal	
Constraints	Max. stress of top spindle < 500MPa	
	Max. stress of end coupling < 500MPa	
Design variables	Top spindle	R1, R2, R3, X1, X2, Ø
	End coupling	T1, L1
	Slipper metal	H1, H2, H3, R1, R2, T

Table 4. Results of optimization for spindle assembly.

<table>
<tr><td rowspan="8">Top Spindle</td><td colspan="4">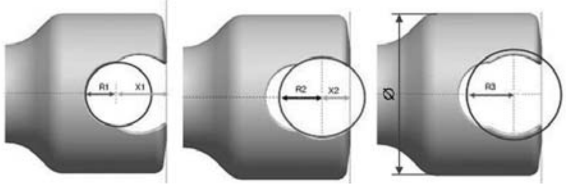
</td><td>Shape of optimal design</td></tr>
<tr><td rowspan="7">Design variable</td><td></td><td>Initial design</td><td>Optimal design</td><td rowspan="7"></td></tr>
<tr><td>R1</td><td>145.0 mm</td><td>150.0 mm</td></tr>
<tr><td>R2</td><td>180.2 mm</td><td>200.0 mm</td></tr>
<tr><td>R3</td><td>205.0 mm</td><td>225.0 mm</td></tr>
<tr><td>X1</td><td>240.0 mm</td><td>320.0 mm</td></tr>
<tr><td>X2</td><td>130.0 mm</td><td>320.0 mm</td></tr>
<tr><td>Ø</td><td>750.0 mm</td><td>856.0 mm</td></tr>
<tr><td rowspan="4">End Coupling</td><td colspan="4">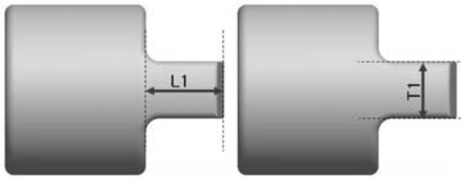
</td><td>Shape of optimal design</td></tr>
<tr><td rowspan="3">Design variable</td><td></td><td>Initial model</td><td>Optimal design</td><td rowspan="3">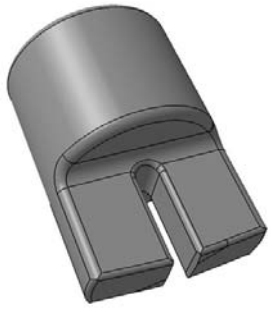</td></tr>
<tr><td>L1</td><td>340.0 mm</td><td>480.0 mm</td></tr>
<tr><td>T1</td><td>250.0 mm</td><td>230.0 mm</td></tr>
<tr><td rowspan="8">Slipper metal</td><td colspan="4">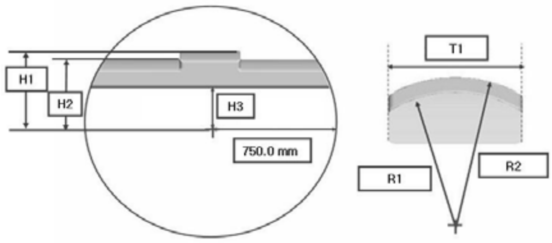
</td><td>Shape of optimal design</td></tr>
<tr><td rowspan="7">Design variable</td><td></td><td>Initial model</td><td>Optimal design</td><td rowspan="7">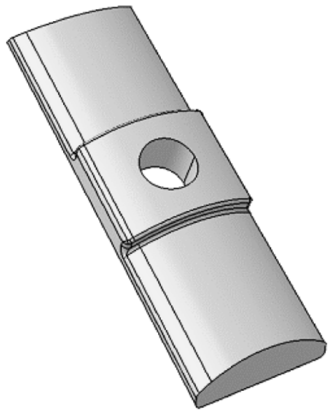</td></tr>
<tr><td>H1</td><td>205.0 mm</td><td>225.0 mm</td></tr>
<tr><td>H2</td><td>180.2 mm</td><td>200.3 mm</td></tr>
<tr><td>H3</td><td>125.0 mm</td><td>115.0 mm</td></tr>
<tr><td>R1</td><td>180.0 mm</td><td>200.0 mm</td></tr>
<tr><td>R2</td><td>203.0 mm</td><td>223.0 mm</td></tr>
<tr><td>T1</td><td>220.0 mm</td><td>240.0 mm</td></tr>
</table>

Fig. 16. Stress contour of the optimized top spindle.

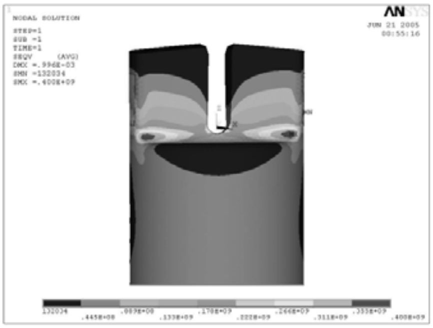

Fig. 17. Stress contour of the optimized end coupling.

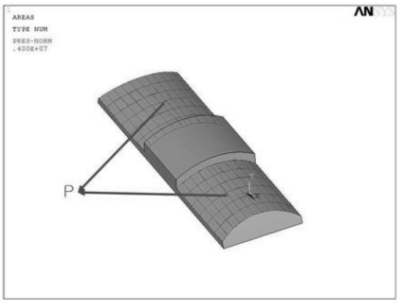

(a) Boundary condition of slipper metal

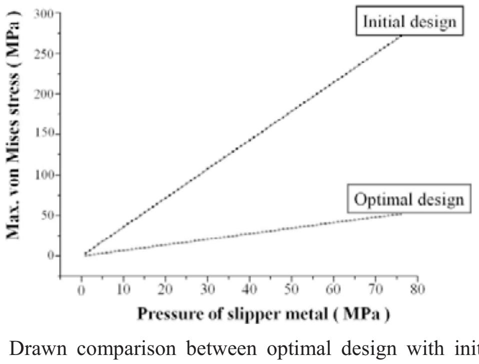

(b) Drawn comparison between optimal design with initial design

Fig. 18. Maximum stress of slipper metal according to uniform distributed load P.

3. Interference check of optimized model

3.1 Space analysis method

A CATIA DMU space analysis is a design checking program which can calculate the interference checking and shortest distance in digital mock-ups[8, 9].

3.2 Interference check under angle with 0°~7.00°

The initial operation of hot mill spindle assembly is set with angle 0°operation angle in horizontal direction. An interference check is performed along the combination type of end coupling and slipper metal. The interference does not occur on the top spindle and slipper metal. Under an operation angle from 2.97° to 5.77° of the top spindle, an interference check is conducted on the contact surface. There is no component which interferes with each other. The maximum operation angle which is used for the hot mill process is 7.00°, and interference checking is preformed. There is not a part which is interfered from interference checking results, so actual operation of the hot mill spindle assembly can operate on the normal operation condition. Fig. 19 shows interference checking area of optimized spindle assembly.

Table 5. Results of interference check for optimized spindle assembly.

Rotation angle	Moving distance	A region tolerance	B region tolerance
0.00˚	0.0 mm	31.5 mm	17.2 mm
2.97˚	14.5 mm	23.8 mm	16.7 mm
5.64˚	52.0 mm	16.5 mm	19.0 mm
5.77˚	55.0 mm	16.1 mm	18.8 mm
6.70˚	73.0 mm	13.5 mm	19.0 mm
7.00˚	80.0 mm	12.7 mm	21.7 mm

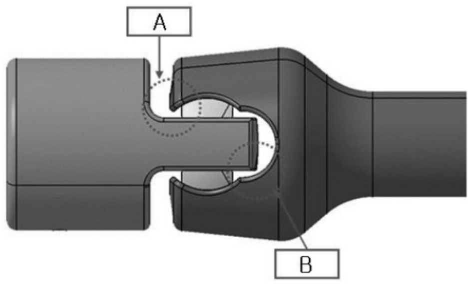

Fig. 19. Interference checking area of optimized spindle assembly.

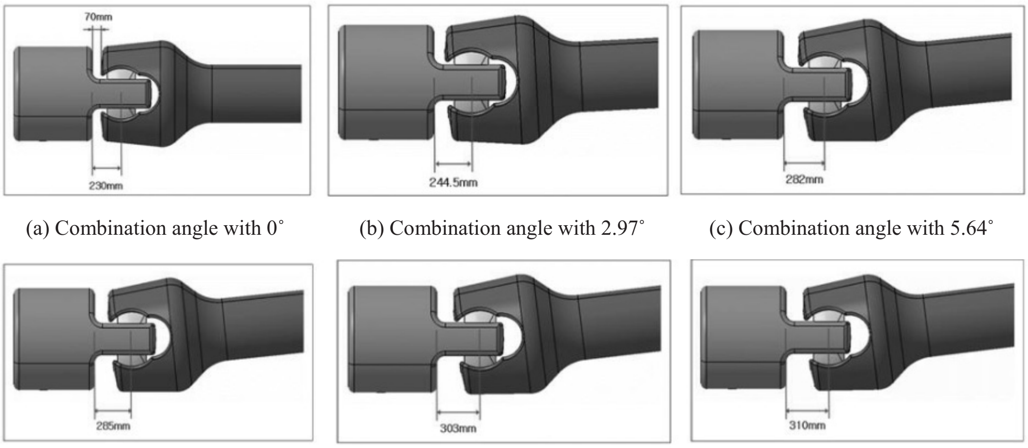

(a) Combination angle with 0˚ (b) Combination angle with 2.97˚ (c) Combination angle with 5.64˚

(d) Combination angle with 5.77˚ (e) Combination angle with 6.70˚ (f) Combination angle with 7.00˚

Fig. 20. Configuration of interference check under combination angle with 0˚~7.00˚.

Configuration of interference check under combination angle with 0°~7.00° is shown in Fig. 20. Results of the interference check for an optimized spindle assembly are shown in Table 5. Moving distance and tolerance of A and B region are presented with rotation angles.

4. Conclusions

The major conclusions of this study are as follows:

(1) The life cycles of slipper metal are reduced by stress concentration of contact surface.
(2) Stress concentration of slipper metal occurred because of contact surface inconsistency.
(3) Combination angle of spindle assembly should be determined considering contact surface consistency of slipper metal.
(4) Maximum stress of optimal slipper metal decreased by 80 percent compared with the initial slipper metal.
(5) Interference of the optimized model does not occur during a combination process and driving process.

References

[1] M. A. Cavliere, M. B. Goldschmit and E. N. Dvorkin, Finite element analysis of steel rolling processes, Computers and Structures, 79 (2001) 2075-2089.

[2] F. C. Minutolo, M. Durante, F. Lambiase and A. Langella, Dimensional analysis of a new type of groove for steel rebar rolling, *Journal of Materials Processing Technology*, PROTEC-9261. 175 (2005) 69-76.

[3] J. Li, R. Sedaghati, J. Dargahi and D. Waechter, De-sign and development of a new piezoelectric linear inchworm actuator, Mechatronics, 15 (2005) 651-681.

[4] C. H. Huang and T. M. JU, The estimation of surface thermal behavior of the working roll in hot rolling process, *Int. J. Heat Mass Transfer* 38 (6) (1995) 1019-1031.

[5] ANSYS MANUAL (Ver.6.0), Swanson Analysis Systems Inc. (2001).

[6] W. Raza and K. Y. Kim, Shape optimization of LMR fuel assembly using radial basis neural network technique, *Transactions of Korean Society of Mechanical Engineers* B 31 (8) (2007) 663-671.

[7] J. W. Chae, Y. S. Lee and T. K. Park, The shape optimization of MIL-S-46119 ring obturator under the high pressure, *Transactions of Korean Society of Mechanical Engineers* A 27 (1) (2003) 1-7.

[8] CATIA Version 5 Release 14 online documentation, Dassaut System, (2005).

[9] S. W. Byun, Y. S. Lee, H. S. Lee and J. J. Lee, Contact damage analysis of hot mill spindle assembly with kinematics simulation, Key Engineering Materials 326-328 (2006) 1121-1124.